Human Molecular Genetics, 2009, Vol. 18, No. 6 *1075–1088*
doi:10.1093/hmg/ddp004
Advance Access published on January 18, 2009

Expression of mutant β2 nicotinic receptors during development is crucial for epileptogenesis

Irene Manfredi[1], Alessia D. Zani[2], Luca Rampoldi[1,3], Simona Pegorini[2], Ilenia Bernascone[1,3], Milena Moretti[4], Cecilia Gotti[4], Laura Croci[1], G. Giacomo Consalez[1], Luigi Ferini-Strambi[5], Mariaelvina Sala[2], Linda Pattini[6] and Giorgio Casari[1,7,8,*]

[1]San Raffaele Scientific Institute, Via Olgettina 58, 20132 Milan, Italy, [2]Department of Pharmacology, Chemotherapy and Medical Toxicology, University of Milan, Via Vanvitelli 32, 20129 Milan, Italy, [3]Dulbecco Telethon Institute, San Raffaele Scientific Institute, Via Olgettina 58, 20132 Milan, Italy, [4]CNR Institute of Neuroscience, Cellular and Molecular Pharmacology, Department of Medical Pharmacology, University of Milan, Via Vanvitelli 32, 20129 Milan, Italy, [5]Sleep Disorders Center, Department of Neurology, San Raffaele Scientific Institute, Via Stamira d'Ancona 20, 20127 Milan, Italy, [6]Department of Bioengineering, Politecnico di Milano, P.za Leonardo da Vinci 32, 20133 Milan, Italy, [7]Vita-Salute University, San Raffaele Scientific Institute, Via Olgettina 58, 20132 Milan, Italy and [8]Istituto Nazionale di Neuroscienze (INN), Via Olgettina 58, 20132 Milan, Italy

Received November 7, 2008; Revised and Accepted December 28, 2008

Autosomal dominant nocturnal frontal lobe epilepsy (ADNFLE) is a focal form of epilepsy characterized by seizures occurring during non-REM sleep. We have developed and characterized the first mouse model for ADNFLE type III carrying the V287L mutation of the β2 subunit of neuronal nicotinic receptor. Mice expressing mutant receptors show a spontaneous epileptic phenotype by electroencephalography with very frequent interictal spikes and seizures. Expression of the mutant β2 subunit is driven by a neuronal-specific tetracycline-controlled promoter, which allows planned silencing of transgene expression in a reversible fashion and tracking the involvement of mutant receptor in crucial phases of epileptogenesis. We found that restricted silencing during development is sufficient to prevent the occurrence of epileptic seizures in adulthood. Our data indicate that mutant nicotinic receptors are responsible for abnormal formation of neuronal circuits and/or long-lasting alteration of network assembly in the developing brain, thus leading to epilepsy.

INTRODUCTION

Epilepsy is one of the most common neurological disorders, affecting 0.5–1% of world population (1). In the last decades a genetic etiology has been confirmed for several epileptic syndromes, caused by mutations in genes coding for subunits of voltage-gated and ligand-gated ion channels (2).

Among these, autosomal dominant nocturnal frontal lobe epilepsy (ADNFLE) was the first idiopathic epilepsy whose genetic origin was elucidated. Hallmarks of ADNFLE are complex seizures arising mainly during non-REM sleep, with age of onset during childhood (3). In most cases, seizures can be controlled by anti-epileptic drugs, however one-third of patients are refractory to treatment (4).

So far, mutations linked to ADNFLE have been identified in genes coding for the α4 (*CHRNA4*) (5–7), α2 (*CHRNA2*) (8) and β2 (*CHRNB2*) (9–11) subunits of the neuronal nicotinic receptor (nAChR). Heteropentameric structures composed of α4 and β2 subunits represent the major subtype of nAChR in brain (12).

Since most of the mutations affect the second transmembrane domain of the subunit that leans into the ion gate of the receptor, their functional effect has been mainly studied through electrophysiological approach by expression of

*To whom correspondence should be addressed at: Vita-Salute San Raffaele University and Human Molecular Genetics Unit, San Raffaele Scientific Institute, DIBIT, Via Olgettina 58, 20132 Milan, Italy. Tel: +39 0226433502; Fax: +39 0226434767; Email: casari.giorgio@hsr.it

© *The Author 2009. Published by Oxford University Press. All rights reserved.*
For Permissions, please email: journals.permissions@oxfordjournals.org

Downloaded from hmg.oxfordjournals.org at (D) Fukuoka U Med on October 4, 2010

reconstituted receptors. Although a common effect of the different mutations is expected, the results obtained by *in vitro* analyses have been often divergent (13,14). Indeed, besides previous findings that reported a loss of function of the receptor due to *CHRNA4* mutations (15), we documented a gain of function when expressing reconstituted receptors carrying the β2 subunit V287L mutation, which we have previously shown linked to ADNFLE (9).

In fact V287L mutant receptors display a dramatic desensitization delay after agonist activation, leading to a prolonged cationic inward current.

Here we describe the first ADNFLE mouse model harboring the V287L missense mutation of the β2 nAChR subunit. *In vivo* studies on α4 ADNFLE knock-in mutant (16,17) have provided information on the mutation effect on receptor function, however, the precise pathogenetic mechanism of this epilepsy is still unknown.

Knock-in models are very informative tools to study this disorder but they may be of limited efficacy, since obtained by permanent genetic modifications, when approaching the onset timing of the disease, which implicates adaptive changes in brain physiology.

We therefore took advantage of the tetracycline-controlled expression system (tet-off), that allows silencing of transgene expression in a reversible fashion, in the effort to dissect the role of mutations in epileptogenesis and epilepsy. This strategy actually enabled us to control temporal expression of mutation, tackling its epileptogenic role during development.

RESULTS

Development of ADNFLE mouse model

In order to study *in vivo* the effects of the V287L mutation, we generated a transgenic mouse model, employing the TET-OFF conditional expression system (18). Briefly, the gene of interest is cloned under control of the tetracycline responsive element (TRE), whose activation is dependent on binding of tetracycline-controlled transcriptional activator (tTA). Binding of tTA to TRE, and consequently transcription of the downstream gene, can be prevented by interaction of tTA with tetracycline.

We introduced the pathogenetic V287L mutation by site-directed mutagenesis into the coding sequence of the murine *Chrnb2* gene. The first intron was maintained to ensure a correct maturation of the transcript. Mutant *Chrnb2*^{V287L} transgene was then cloned into pUHD10.3 vector, in between the TRE and the polyadenylation sequence of SV40, generating the final construct, pTetO-β2VL (Fig. 1A). Regulated expression of pTetO-β2VL was confirmed in cells before transgenesis (Fig. 1B), then the transgene was microinjected into fertilized eggs of FVB strain mice to obtain FVB-Tg(TRE-*Chrnb2*^{V287L}) responder mice. By PCR screening of the progeny, we identified three founders, which generated three lineages, called FVB-Tg(TRE-*Chrnb2*^{V287L})H1, FVB-Tg(TRE-*Chrnb2*^{V287L})H3 and FVB-Tg(TRE-*Chrnb2*^{V287L})H5 (hereinafter H1, H3 and H5 responder lines). Since both the heteromeric β2 nAChRs and the prion protein have a broad and overlapping expression in central nervous system (CNS), responder mice of H1, H3 and H5 lines were crossed with a line of transgenic mice

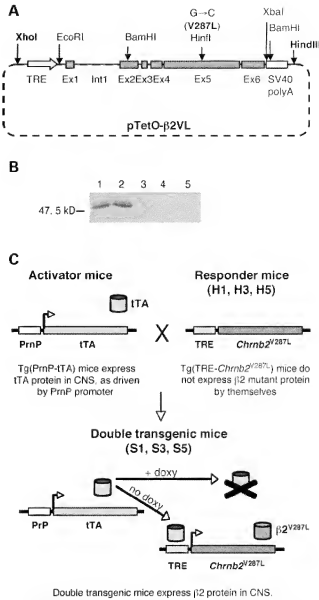

Figure 1. Transgenic constructs. (**A**) Schematic map of pTetO-β2VL construct. The coding sequence of mouse *Chrnb2* gene (exons 1–6), comprising the first intron, was mutagenized to obtain the V287L ADNFLE mutation, thus cloned down-stream the TRE and up-stream the SV40 polyadenylation sequence (SV40 polyA). The V287L missense mutation inserts a new *HinfI* restriction site that is absent in wild-type *Chrnb2* gene. (**B**) pTetO-β2VL expression test. In the presence of pUHD15.1 plasmid that expresses the activator protein tTA, mutant β2 subunit (52 kD) was correctly expressed (lane 1), while it was not in the absence of tTA (lane 3). By adding doxycycline (1 μg/ml in culture medium for 48 h), which inhibits tTA binding to TRE promoter, expression is completely silenced (lanes 4–5). Co-expression of wild-type α4 subunit did not influence the stability of β2 mutated subunit (lanes 2, 3 and 5). (**C**) Schematic diagram of tet-off system. *Chrnb2*^{V287L} transgene was excised from pTetO-β2VL construct with *XhoI* and *HindIII* enzymes, and then injected into FVB fertilized eggs generating three lines of transgenic responder mice (H1, H3 and H5 lines) that do not express transgene *per se*. To achieve activation of TRE promoter by tTA, responder mice were bred with transgenic activator mice, expressing tTA driven by PrnP promoter. S1, S3 and S5 double transgenic lines express mutant β2 subunit in CNS. Administration of doxycycline silences expression of *Chrnb2*^{V287L} transgene.

Downloaded from hmg.oxfordjournals.org at (D) Fukuoka U Med on October 4, 2010

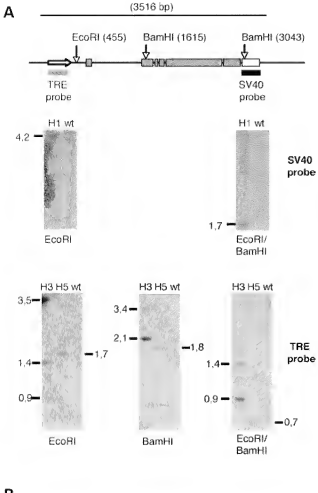

expressing tTA under the control of the prion protein promoter (FVB-Tg(PrnP-tTA/F959) (19), ensuring a CNS-specific expression from embryonic stages and persisting throughout the adult life (20).

However, the expression of the mutant transgene under heterologous PrnP regulatory sequences is not expected to result in the ectopic expression of the receptor. In fact, the assembling of the pentameric functional receptor requires the presence of nicotinic partner subunits, which are normally expressed in specific neuronal cells together with proper chaperone machinery to traffic to the surface.

After crossing we obtained three lines of double transgenic mice (dtg), carrying both *Chrnb2*^{V287L} and tTA transgenes that we named FVB-Tg(tTA:*Chrnb2*^{V287L})S1, FVB-Tg (tTA:*Chrnb2*^{V287L})S3 and FVB-Tg(tTA:*Chrnb2*^{V287L})S5, respectively; hereafter, for short, S1, S3 and S5 mice (Fig. 1C).

Transgenic mice of S1, S3 and S5 lines were viable and fertile. No significant differences in the sensory-motor functions were observed between transgenic and wild-type mice by SHIRPA protocol primary screening as described in methods (data not shown).

Transgene genomic integration

Tg(*Chrnb2*^{V287L}) integral insertion was assessed in responder lines (H1, H3 and H5) by Southern blot hybridization analysis, using probes at 5' (on TRE promoter) and 3' (on SV40 polyadenylation sequence) of the transgene. Detection of a single hybridization band demonstrated that in H1 and H5 lines the transgene was inserted in single copy. Conversely in H3 line the complex pattern of bands observed indicated a tandem insertion of multiple copies (Fig. 2A). In fact we determined that the H3 line carries four copies of the transgene arranged in tandem (Fig. 2B).

The exact insertion site of the transgene was also defined in each line through inverse PCR to ensure that the phenotype observed in double transgenic mice was specifically due to

Figure 2. Southern blot analysis. (**A**) gDNA from H1, H3 and H5 responder mice was digested with *Eco*RI and/or *Bam*HI restriction enzymes (restriction sites position is given in brackets). Analysis with SV40 probe is shown for H1 line: a single band was detectable in single and double digestion, demonstrating that transgene is inserted in single copy. Band resulting from *Bam*HI single digestion was not detectable. Analysis with TRE probe is shown for H5 and H3 lines: single and double digestions of H5 gDNA show a single band, demonstrating that transgene is inserted in single copy. H3 gDNA digestion shows a complex pattern of bands: the high intensity bands at 3.5 kb in *Eco*RI digestion, at 2.1 kb in *Bam*HI digestion and at 0.9 kb in double digestion are the result of digestion and hybridization of tandem insertion of multiple copies. Wild-type (wt) digested gDNA was loaded as negative control of probe specificity. (**B**) Determination of transgene copy number. gDNA digestion with *Dpn*II enzyme and hybridization with an exon 5 probe allowed direct intra-lane comparison between endogenous gene (band size: 1747 bp) and transgene (band size: 1143 bp). Increasing amounts (2, 4 and 8 µg) of digested gDNA were loaded on agarose gel to mimic 2, 4 and 8 copies of the gene (wild-type 4 µg lane was not loaded). In H3 lanes, bands corresponding to *Chrnb2*^{V287L} transgene show a doubled intensity compared with endogenous gene's bands, suggesting that in H3 line about four copies of the transgene were inserted.

Downloaded from hmg.oxfordjournals.org at (D) Fukuoka U Med on October 4, 2010

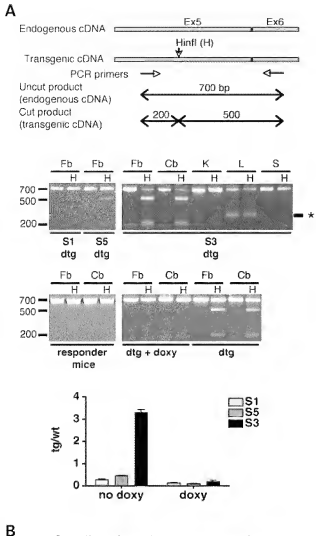

expression of *Chrnb2*^{V287L} transgene and not to its insertion in genomic regions coding for proteins involved in neuronal physiology. Actually transgenes were inserted in non-coding regions of the genome (H1 in chr18:36994820; H5 in chr11:21926392; H3 in chr1:12,085,938) and did not alter expression of the genes in *cis*.

In particular, in the H3 line we mapped transgene insertion in intron 20 of *Ehbp1* gene, thus we verified by semiquantitative RT–PCR that *Ehbp1* gene expression was not altered in H3 transgenic line (see Supplementary Material).

Chrnb2^{V287L} transgene expression

The *Chrnb2*^{V287L} transgene does not include N- or C-terminus tag to avoid potential aberrant behavior of the encoded protein; this, however, hampers the discrimination between endogenous and transgenic β2 proteins. Analysis of transgene expression was therefore performed on the relative mRNAs. Transgenic and endogenous β2 cDNAs differ for the presence of a restriction site that allows the relative quantization. mRNAs from several different tissues confirmed the stable and neuronal specific expression of transgene (Fig. 3A). Complete silencing of transgene expression was confirmed in mice treated with the tetracycline analogue doxycycline (Fig. 3A). The brain regional expression of Tg(*Chrnb2*^{V287L}) was also analyzed. We observed that the regional expression of transgene was higher in cortex, hippocampus, cerebellum and caudate-putamen. S3 mice showed the highest expression compared with S1 and S5 mice, as expected for the multiple copy insertion (Fig. 3B). Probably due to a position effect (21), S1 line expresses the transgene to a lower level than S5, though both lines integrated a single copy of the transgene.

β2 protein expression level is higher in S3 mice, as expected from transcriptional data, in cortex, caudate-putamen and hippocampus. We found unchanged level of β2 subunit in the thalamus and, importantly, of α4 subunit in all CNS areas (Fig. 4A–C). We thence verified that the increase in β2 sub-

Figure 3. Transgene expression analysis. (**A**) Endogenous and transgenic *Chrnb2* cDNA (700 bp PCR product) was amplified with primers on exons 5 and 6. With a subsequent digestion with *Hin*fI enzyme, specific for the transgene, the uncut product derived from endogenous gene amplification (700 bp) could be distinguished on electrophoresis gel from fragments derived from amplified and digested transgenic cDNA (500 and 200 bp). Each sample was loaded on gel as indigested PCR product and *Hin*fI digested (H). S1, S5 and S3 double transgenic mice (dtg) expressed the mutated β2 subunit in neuronal tissues, while in the absence of rtA (responder mice and non neuronal tissues) the transgene was not expressed. Transgene expression was correctly silenced in dtg mice ($n = 3$ for each line) by administration of doxycycline (+doxy). S3 mice show the highest level of expression. * indicates an aspecific band at ≈250 bp, that appears stochastically. Histogram shows transgene level of expression normalized on endogenous' in basal conditions and after doxy treatment (mean ± s.d., $n = 3$). Fb, forebrain; Cb, cerebellum; K, kidney; L, liver; S, spleen. (**B**) Transgene brain regional expression was assessed in S1, S5 and S3 mice. Gel loaded with S3 samples is shown. Transgene expression follows endogenous gene's expression pattern. S1, S5 and S3 mice express increasing levels of transgene, respectively, as shown in graph (mean ± s.d., $n = 3$). Cx, cortex; Th, thalamus; CPu, caudate-putamen; Hip, hippocampus; Hy, hypothalamus; Cb, cerebellum; Bst, brainstem.

Downloaded from hmg.oxfordjournals.org at (D) Fukuoka U Med on October 4, 2010

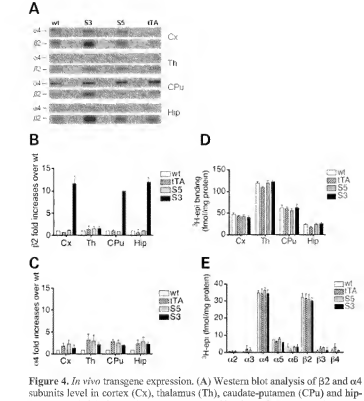

Figure 4. *In vivo* transgene expression. (**A**) Western blot analysis of β2 and α4 subunits level in cortex (Cx), thalamus (Th), caudate-putamen (CPu) and hippocampus (Hip) for each genotype. Quantification of β2 (**B**) and α4 (**C**) subunit protein expression in wild-type, tTA, S3 and S5 lines. (mean values ± s.e.m.). Data are expressed as fold increase of optical density relative to wild-type. Higher expression of β2 subunit was observed in cortex, hippocampus and caudate-putamen of S3 mice, but not in thalamus, as expected on the basis of RT–PCR. No significant increase in α4 subunit level was observed in mutant mice compared to controls. (**D**) Receptor binding analysis by ^{3}H-epibatidine (^{3}H-epi) to detect β2 containing nAChR subtypes. Values are expressed as fmol of specific labeled ^{3}H-epi binding sites per mg of protein, and are the mean values ± s.e.m. of four experiments performed in triplicate for the different genotypes. No significant differences in the total number of nicotinic receptors were found. (**E**) ^{3}H-epi-labeled nAChRs were immunoprecipitated from cortical membranes with specific α2, α3, α4, α5, α6, β2, β3, β4 antibodies. Results are expressed as fmol of ^{3}H-epi-labeled receptors per mg of protein, and are the mean values ± s.e.m. of three experiments performed in duplicate for the different genotypes. No significant differences in nAChR subtypes composition were found.

units amount did not lead to a higher number of assembled receptors, since it could cause increased neuronal excitability irrespectively of the mutation.

Epibatidine, a high affinity agonist of α4-β2 receptors, is typically used in heteromeric nAChRs binding experiments. We checked the binding affinity of epibatidine to the mutant receptor by co-transfecting constructs expressing α4 and wild-type β2 or α4 and V287L β2 subunits into HeLa cells. No difference in affinity for ligand was observed between wild-type and mutant receptors (wild-type $K_D = 98$ pM, CV = 29%; mutant $K_D = 100$ pM, CV = 24%; wild-type $K_i = 17.1$ nM, CV = 38%; mutant $K_i = 14.9$ nM, CV = 28%).

We therefore proceeded to the estimation of the total number of β2-containing nAChRs by binding of ^{3}H-epibatidine to membranes obtained from cortex, hippocampus, caudate-putamen and thalamus of wild-type (wt), transgenic tTA, S3 and S5 mice (Fig. 4D). No significant difference was found among the different strains. As expected nor ^{125}I-α-Bungarotoxin binding of homomeric receptors was different (data not shown). These data ensure that the phenotype observed in mutant mice is exclusively determined by incorporation of mutant β2 subunits in functional receptors and not by an increased receptor number.

Moreover we verified that the relative subunit composition of assembled receptors was not altered in mutant mice by immunoprecipitation assay with subunit-specific antibodies and ^{3}H-epibatidine labeled nAChRs on cortical tissues (Fig. 4E).

Basal brain electrical activity

The most commonly used protocols for detection of spontaneous seizures in animal models are based on repeated electroencephalographic (EEG) recordings of animals for few hours a day, however, those could be uninformative being limited to specific times of the day. In order to rule out the occurrence of spontaneous seizures in our transgenic model, we decided to perform continuous EEG recordings of each animal for 24 h. EEG traces were analyzed with an unsupervised computerized algorithm, that allowed an unbiased detection and quantification of EEG abnormalities, and histograms of amplitude were derived from each recording (see Materials and Methods).

We observed that transgenic mice of both S3 ($n = 15$) and S5 ($n = 13$) lines displayed a sharp epileptic phenotype characterized by very frequent spikes of high amplitude and spontaneous seizures (Fig. 5A) during the 24-h recordings. Such abnormal EEG was never observed in control animals (wild-type, $n = 14$ and tTA, $n = 13$), while it was observed only in one out of eight S1 mice (typical histograms obtained from transgenic and control mice are shown in Fig. 5B).

Analysis of the occurrence of EEG abnormalities in transgenic mice showed a gradient of severity of the phenotype correlated with the level of expression of the transgene. Indeed mice of S3 line analyzed by EEG recording showed spontaneous seizures, 3–21 episodes (seven on average) during 24 h, each lasting 15–40 s (25 s on average), while S5 mice more rarely displayed brief spontaneous seizures (2–3/24 h), lasting 1–8 s of duration (3.8 s on average), even though they manifested very frequent interictal spikes of high amplitude in each session of recording (Fig. 5C). The absence of an epileptic phenotype in S1 mice could therefore be explained with the very low level of transgene expression observed.

These results prove that expression of human ADNFLE gain-of-function V287L mutation in mice leads to a spontaneous epileptic phenotype, whose penetrance and severity is dependent on gene dosage.

Power spectrum of basal EEG recordings was also analyzed and, in particular, we focused on delta (0.5–4.0 Hz) and theta (4.0–8.0 Hz) waves, since those rhythms are typically prevalent during distinct phases of sleep. We observed that in transgenic mice of all three lines there was a predominance of delta rhythm, while in control mice theta rhythm was more represented during 24 h recordings ($P < 0.01$). Moreover the epileptic events observed in S3 and S5 mice occurred mainly during epochs of increased delta activity ($P < 0.05$) (Fig. 6). Analogously to the human disease, most of the seizure

Downloaded from hmg.oxfordjournals.org at (D) Fukuoka U Med on October 4, 2010

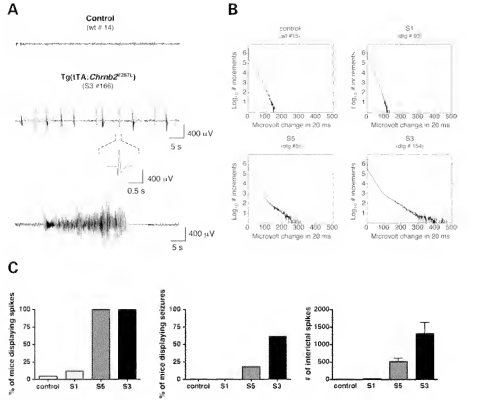

Figure 5. EEG basal recordings. (A) 1 min of EEG traces from control and S3 transgenic mice is shown. Transgenic mice of S5 and S3 lines display abnormal EEG with frequent spikes of high amplitude and spontaneous seizures. (**B**) Inerements detected by unsupervised algorithm during every 24 h recording were plotted in histograms of rectified increments amplitude on a log scale (see Materials and Methods). Here are shown representative histograms derived from 24 h recordings of a mouse baseline EEG for each genotype. In control and S1 mice that do not display EEG abnormalities, the histogram falls off logarithmically with amplitude. In S5 and S3 mice frequent interictal spikes and seizures produce an excess of high amplitude fast EEG increments, thus the histogram decays slower; in a log-linear plot it deviates from the exponential distribution. Values outside the exponential distribution expected for normal EEG were identified as spikes. (C) Severity of the phenotype displays apparent gene-dosage dependence. Left histogram shows the percentage of mice displaying interictal spikes; the middle histogram shows the percentage of mice displaying complex seizures; right histogram shows mean ± s.e.m. of the number of interictal spikes counted for each animal in 24 h recordings. S3 mice show the most severe phenotype, displaying frequently seizures during 24 h recording and a higher number of interictal spikes.

episodes of both S3 and S5 mutants took place during the light period (75%), which corresponds to murine resting–sleeping phase.

EEG recordings after transgene silencing

Inducible models are particularly useful for potentially reverting the phenotype. In order to test whether transgene silencing could revert the epileptic phenotype of transgenic animals, we treated adult mice of S3 ($n = 7$) and S5 ($n = 5$) lines with oral doxycycline. EEG recordings were performed for 24 h both before (basal EEG) and after chronic doxycycline treatment. Despite a complete silencing of transgene expression, S5 and S3 mice still displayed unchanged and very frequent interictal spikes and seizures associated with increased delta power (Fig. 7), indicating that the established epileptic phenotype could not be reverted by simply silencing the expression of the mutant allele. No amelioration of epilepsy, neither in number of events or seizure duration, was observed in adult mice after chronic anti-epileptic treatment with carbamazepine (data not shown) administered at the dose of 30 mg/kg, which is in the high range of efficacy in rodents (22).

We hypothesized that the observed irreversibility of the epileptic phenotype could stem from permanent alterations of neural circuits. In particular, we concentrated on the possibility that mutant nicotinic receptors could affect connectivity or synaptogenesis, resulting in long-lasting abnormalities. We therefore tested the effect of transgene silencing during developmental stages on the epileptic phenotype. We focused on S3 line mice, since they display the most severe phenotype. Treating pregnant females with doxycycline from day one postcoitum, we could achieve complete expression silencing within the earliest expression of functional receptors, since the drug can cross the placenta and can be administered to pups from embryonic day 1 (E1). Treatment was carried on until post-natal day 15 (P15), being doxycycline transferred to pups through maternal milk, in order to maintain the transgene silenced during the stages of brain development in which nAChRs are critically involved, and to grant a fast reactivation upon drug withdrawal. In fact, long lasting silencing may occur after excessively prolonged treatments (23).

It is important to underline that mutant mice retained expression of the endogenous gene when treated with doxycycline from E1 to P15, being thus identical to wild-type mice,

Downloaded from hmg.oxfordjournals.org at (D) Fukuoka U Med on October 4, 2010

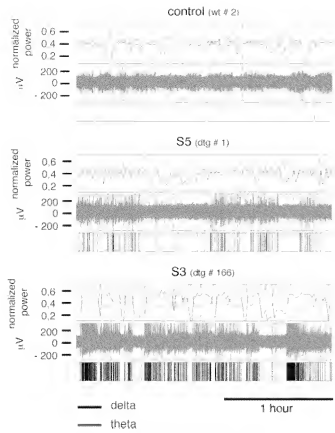

Figure 6. Spectral analysis of EEG recordings. About 2 h of typical EEG recordings from control, S5 and S3 mice are shown with relative spectral analysis. The upper box represents the contribution of delta (black line) and theta (red line) waves, as percentage on the total spectrum, sampled every minute; in the middle box is shown the EEG trace; on the bottom, bars represent spikes and seizures detected automatically. While control mice usually show a predominant theta activity during the 24 h of recording, transgenic mice show a higher delta rhythm. The vast majority of epileptic events occur during epochs of increased delta rhythm.

while termination of treatment allowed a prompt re-expression of the mutant subunit.

Mice underwent EEG recording in adulthood at 4–5 months of age ($n = 4$). Intriguingly we never observed any epileptic event, neither high amplitude spikes nor seizures, even after extensive doxycycline wash out. EEG traces were indeed comparable with those produced by controls (Fig. 8A) showing also a prevalent theta rhythm (Fig. 8B). The correct reappearance of transgene expression was verified at transcription level (Fig. 8C).

These observations indicate that silencing of mutant nicotinic receptor expression during critical stages of brain development is sufficient to prevent the onset of epilepsy in adult mice. This is the first time that a developmental role of mutant nicotinic receptors in epileptogenesis has been proved.

DISCUSSION

Nicotinic receptors influence a variety of physiological processes, including cognitive functions, anxiety, arousal and sleep (24) mainly by regulating neurotransmitter release at the pre-synaptic terminal of neurons (25), although a signal transduction role at post-synaptic or non-synaptic sites has been also recognized (26).

In the past years, mutations in genes coding for subunits of the nAChR have been linked to a specific form of focal epilepsy, ADNFLE (reviewed in 27), and extensive efforts have been made to identify the precise pathogenetic role of mutant receptors with both *in vitro* and *in vivo* approaches.

So far two mouse models expressing S252F and insL264 mutations of *Chrna4* gene have been generated. Both mutants developed on C57BL/6J background exhibit abnormal cortical EEG, associated with increased delta and theta activity, which is normalized by picrotoxin, a $GABA_A$ antagonist (16). Also, cortical slices display increased inhibitory post-synaptic currents after nicotine stimulation, suggesting that abnormal synchronization of pyramidal neurons could determine the occurrence of seizures. However, S252F knock-in model on a mixed CD1-129/Sv genetic background displays no spontaneous seizures, while low doses of nicotine elicit dystonic behavior similar to motor features of human ADNFLE attacks, never accompanied by EEG epileptiform changes (17). The discrepancy between the two S252F models is probably due to the influence of different genetic backgrounds.

The major limitation to the use of *knock-in* models is the irreversibility of the genetic modification. In order to overcome this limitation and challenge the reversibility of the epileptic phenotype, we developed an ADNFLE mouse model expressing the β2 V287L mutation in a tetracycline-inducible fashion.

Continuous EEG recordings revealed a manifest abnormal brain electrical activity in transgenic mice, characterized by very frequent interictal spikes of high amplitude and spontaneous seizures. EEG abnormalities were completely absent in control animals, as well as in mice carrying the transgene without the tTA transcriptional activator, thus witnessing that the epileptic phenotype was exclusively due to expression of the mutant allele. In particular S3 mice, which express the mutant subunit at the highest level, showed the most severe phenotype, displaying frequent spontaneous seizures and interictal spikes. Our results enable us to demonstrate that the epileptic phenotype is specifically due to V287L mutation with a gene-dosage effect, where higher transgene expression corresponds to a relative higher presence of mutant nAChRs, without affecting the total number of nAChRs. In fact, binding experiments have shown no change in the density of receptors among transgenic and wild-type mice.

Several reports demonstrated the interdependence of α4 and β2 subunits expression (28). As expected, the expression of the α4 subunit in our mutant mice is unaffected, further confirming the unaltered number of receptors and possibly excluding ectopic expression of mutant receptors. Moreover, immunoprecipitation experiments excluded alterations of nAChRs subtype composition, thus indicating that higher expression level of mutant β2 subunits neither influence the expression of other nAChR isoforms nor the subunit specificity of the accessory position of the pentamer (28,29). The high expression level of the mutant subunit presumably facilitates incorporation of mutant instead of wild-type subunit into functional receptors with no change in $\alpha4\beta2^*$ receptor stoichiometry.

Downloaded from hmg.oxfordjournals.org at (D) Fukuoka U Med on October 4, 2010

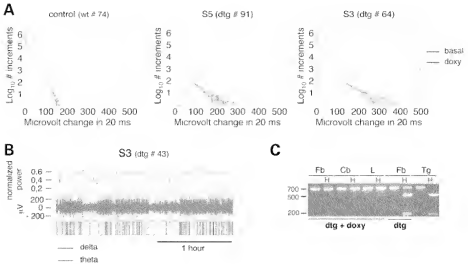

Figure 7. *Chrnb2*^{V287L} transgene silencing is not sufficient to revert the epileptic phenotype. Complete silencing of transgene expression by doxycycline administration (1 mg/ml in drinking water for 1–3 weeks) in adult S5 ($n = 5$) and S3 ($n = 7$) mice was not sufficient to revert the epileptic phenotype. High amplitude spikes and seizures, here shown as histogram deviating from the exponential distribution, were still present in treated adult mice (**A**). Spectral analysis revealed an increased delta rhythm associated with epileptic events (**B**). Confirmation of complete silencing by RT–PCR after recordings is shown in (**C**) (dtg+doxy); RT–PCR on RNA from untreated mice (dtg) was loaded as comparison.

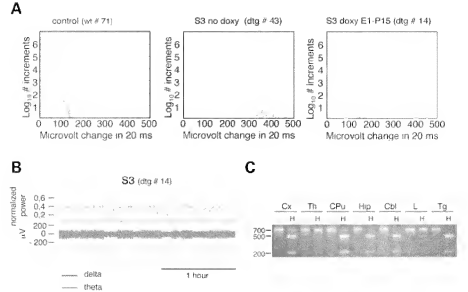

Figure 8. Embryonal *Chrnb2*^{V287L} transgene silencing inhibits the development of epilepsy. (**A**) No epileptic events were detected in 4 months aged mice ($n = 4$) in which transgene expression was silenced during development (S3 doxy E1–P15). Typical histograms of a control mouse and S3 mouse never treated with doxycycline (S3 no doxy) are shown as comparison. Traces of mice treated with doxycycline during development events were completely comparable to control mice traces, showing also a prevalent theta rhythm (**B**). Correct switch on of the transgene was verified by RT–PCR after recording (**C**).

By analyzing the power spectrum of EEG recordings, we interestingly observed that while control mice showed a predominant theta rhythm, transgenic mice displayed a prevalence of delta waves during the 24 h. Moreover we observed a tight correspondence between EEG abnormalities and delta rhythm, as most of spikes and seizures occurred during delta activity.

Activity in the delta frequency range is characteristic of slow wave sleep (30). During wakefulness, thalamic relay neurons that are interconnected with cortex fire with single spikes in a tonic mode; conversely, during sleep inhibitory action of reticular thalamic interneurons on thalamic relay neurons induces an oscillatory mode of firing in thalamo-cortical circuit. Oscillatory firing is sustained by cortico-thalamic efferents providing a positive feedback to reticular nuclei, thus firing of thalamic and cortical neurons get synchronized (31) and involves wider brain areas as sleep deepens (i.e. non-REM sleep stage 3 and 4). EEG delta activity reflects this high degree of synchronization, which is assumed to facilitate the transition to paroxysmal discharges in susceptible brains (32).

Downloaded from hmg.oxfordjournals.org at (D) Fukuoka U Med on October 4, 2010

We suggest that the increased delta activity promotes epileptic events in our transgenic mice. Indeed a correlation between slow-wave sleep and interictal spikes have been demonstrated both in patients with partial epilepsies and in experimental models (32–34), and in particular it has been shown that in ADNFLE patients seizures occur mainly during prominent delta rhythm (35).

Brain electrical activity of transgenic animals was also analyzed after transgene silencing by chronic doxycycline treatment to test the possibility to revert the phenotype. Surprisingly enough, the silencing of mutant nAChRs is not sufficient to abolish seizures once those are established, as we observed an unchanged epileptic activity both in S3 and S5 mice, though the transgene repression of expression was confirmed.

Carbamazepine, a known antiepileptic compound used for the treatment of ADNFLE, failed to produce any amelioration. However, one-third of ADNFLE patients are refractory to antiepileptic treatment (35,36).

The results obtained in our model with doxycycline and carbamazepine treatments point to a non-reversibility of the epileptic phenotype, which could be due to permanent neuronal or circuit alterations. Actually intractable epilepsy can result from alterations of normal cortical development or through formation of abnormal connections or neuronal/synaptic defects (37,38).

We reasoned that if disruption of normal development driven by mutant receptors is the primary cause of epilepsy, then silencing of transgene expression during development stages should prevent its occurrence.

Actually when we repressed the mutant β2 transgene expression from E1 to P15 in S3 mice, they failed to display any epileptic phenotype in adulthood, demonstrating that silencing of the transgene during development is sufficient to prevent initiation of the epileptic phenotype.

The role of nicotinic receptors in neuronal development has been demonstrated by *in vitro* and *in vivo* evidence (39). In fact, β2 and other nAChRs subunits are expressed very early in development (40,41) and nAChRs activation induces early gene expression through calcium permeation (42), hence indicating a pivotal role in the maturation of central circuits. A morphogenetic role has also been postulated since acetylcholine can affect axon growth and pathfinding, and induce a positive turning response, by acting on nAChRs (43). In different models, the complete loss of function of the β2 subunit gene causes an abnormality of the visual system functional organization (44) and of passive avoidance behavior in adulthood (45). Fine control of circuits wiring by β2 and α7 containing receptors has also been demonstrated in developing hippocampus (46). Moreover, recently a crucial role of nicotinic receptors has been shown during early development in the modulation of GABAergic transition from excitatory to inhibitory and in synaptogenesis and maturation of neuronal circuits through cooperation with inhibitory GABA (47).

However, no evidence of macroscopic brain malformation was observed in our transgenic mice. We suggest that mutant nicotinic receptors determine altered formation of neural circuits and/or altered synaptogenesis, leading to long-lasting modifications of network tuning, resulting directly in an epileptic phenotype or creating a favorable environment for further epileptogenic insults (48).

A developmental origin of ADNFLE has been hypothesized for its onset in childhood (49,50). We report for the first time a link between neural networks development and ADNFLE in our conditional model, which associates an epileptic phenotype with the conditional expression of mutant receptor and provide a unique tool for further investigation of ADNFLE molecular pathogenesis.

MATERIALS AND METHODS

Reagents and suppliers

All chemicals and drugs were obtained from Sigma-Aldrich (Milan, Italy), if not otherwise indicated. Restriction enzymes, T4 ligase and buffers were obtained from New England Biolabs (Ipswich, MA, USA). *Taq* polymerase (HotMaster *Taq* Polymerase) and buffer were obtained from Eppendorf (Hamburg, Germany).

All reagents were used according to manufacturer instructions.

Subunit-specific polyclonal antibodies were developed in Dr Cecilia Gotti' s laboratory (Institute of Neuroscience-CNR, Milan, Italy) as previously described (51).

Transgenic construct generation

Chrnb2^{V287L} transgene was obtained with two steps of amplification: first, FVB strain genomic DNA (gDNA) was amplified by polymerase chain reaction (PCR) with *Pfu* DNA polymerase (Promega, Madison, WI, USA) using forward primer (CGGAATTCCGGCTTCAGCACCACGGACAGC, *Eco*RI tail) on exon 1 and reverse primer on exon 2 (CTGA TGAGCTGTGCCAATGATACC) of *Chrnb2* gene (Fragment 1) at 94°C for 2 min, 34 cycles at 94°C for 45 s, 62°C for 45 s, 72°C for 2 min and 30 s and 72°C for 10 min; then first strand cDNA was amplified with forward primer (GTCACAGAG GAGCGGCTGGTGG) on exon 2 and reverse primer on exon 6 (GCTCTAGAGGGTGAGGAGCTGCAAATGAGAG, *Xba*I tail) (Fragment 2) using *Pfu* DNA polymerase at 94°C for 2 min, 10 cycles at 94°C for 45 s, 68°C for 45 s, 72°C for 2 min and 30 s, 24 cycles at 94°C for 45 s, 68°C for 45 s, 72°C for 2 min and 30 s and 72°C for 10 min. Fragment 1 (1263 bp) was digested with *Eco*RI and *Bam*HI, and then cloned into pBluescript SK(+) vector (Stratagene, La Jolla, CA, USA). Fragment 2 (1453 bp) was digested with *Bam*HI and *Xba*I, cloned into another pBluescript SK(+) vector (Stratagene) and then mutagenized (QuickChange^{TM} Site-Directed Mutagenesis Kit, Stratagene) to insert human ADNFLE V287L mutation into exon 5. Both fragments were then excised from vectors and cloned together into with *Eco*RI–*Xba*I opened pUHD10.3 vector (developed by Prof. H Bujard, University of Heidelberg, Germany) to obtain pTetO-β2VL construct.

Transient transfections of pTetO-β2VL construct in HEK293 cells, with or without pUHD15.1 vector (17) expressing tTA and pcDNAα4 vector expressing human α4 nAChR subunit, were performed by calcium-phosphate.

Cells were collected after 40 h and lysed in 1% NP40, 50 mM Tris pH 7.5, 150 mM NaCl. Equal amounts of protein extracts (70 μg) were loaded on SDS–PAGE. Transblotted

Downloaded from hmg.oxfordjournals.org at (D) Fukuoka U Med on October 4, 2010

nitrocellulose membranes were incubated with antibody against mouse β2 subunit followed by incubation with horseradish peroxidase-conjugated secondary antibody (Promega, Madison, WI, USA; 1: 3000). Protein bands were visualized with the Enhanced Chemiluminescence kit (Amersham Biosciences, Piscataway, NJ, USA). In experiments of transgene silencing, doxycycline was added to cells medium at 1 μg/ml and cells maintained in doxycycline for 48 h.

Mice lines

Chrnb2^{V287L} transgene excised from pTetO-β2VL construct with *Xho*I–*Hin*dIII enzymes was microinjected into pronuclei of FVB fertilized oocytes (the procedure was developed in San Raffaele Core Facility for Conditional Mutagenesis, CFCM). Progeny's genotype was screened by PCR to identify Tg(TRE-*Chrnb2*^{V287L}) positive mice. Briefly, gDNA extracted from tail biopsy was amplified with two different pairs of forward and reverse primers: Tetfor2 (CGGGTCGAGGTAGG CGTGTA) on TRE promoter with f1r1rev1 on intron 1 (GCG TTATCTCAACCCTCTTGCCA), specific for the transgene (599 bp product) and mb2f2for2 (GACACAGAGGAGCGGC TGGTGG) on exon 2 with f2r2rev2 (CTTCTCCAGGAAGA CCACCTTG) on exon 6 to obtain a 948 bp PCR product for the transgene and 2371 bp for the *Chrnb2* endogenous gene. Both PCRs were performed at 94°C for 1 min and 30 s, 36 cycles at 94°C for 25 s, 62°C for 30 s, 65°C for 50s and 65°C for 10 min. The three founders identified were backcrossed with FVB mice to generate corresponding responder lines.

Crossing of Tg(TRE-*Chrnb2*^{V287L}) responder mice with Tg(PrnP-tTA/F959) mice (kindly provided by S.B. Prusiner, University of California, San Francisco, USA) generated Tg(tTA:*Chrnb2*^{V287L}) mice, whose genotype was screened by two PCRs using mβ2f2for2-f2r2rev2 primers on *Chrnb2*^{V287L} transgene (as described earlier) and tTAfor (TAACAACCCG TAAACTCGCC) with tTArev (AAGTAAAATGCCCCACA GCG) primers on tTA transgene (PCR product: 351 bp) at 94°C for 1 min and 30 s, 34 cycles at 94°C for 25 s, 55°C for 20 s, 65°C for 45s and 65°C for 10 min.

All the behavioral analyses were conducted on Tg (tTA:*Chrnb2*^{V287L}) mice, using wild-type and Tg(PrnP-tTA) littermates as controls.

Animals were housed in SPF conditions, maintained on a 12-h light/dark cycle, with free access to food and water. All procedures involving animals and their care were conducted in conformity with guidelines of the Institutional Animal Care and Use Committee, San Raffaele Hospital, Milan, Italy, in compliance with national (D.L. No. 116, G.U. Suppl. 40, Feb. 18, 1992, Circolare No. 8, G.U., 14 Lug. 1994) and international laws and policies (EEC Council Directive 86/609, OJ L 358, 1 DEC. 12, 1987; NIH Guide for the Care and use of Laboratory Animals, U.S. National Research Council, 1996).

Analysis of transgene genomic integration

gDNA extracted from tails of Tg(TRE-*Chrnb2*^{V287L}) responder mice and wild-type control mice, was digested over/night with an excess of *Eco*RI and/or *Bam*HI enzymes and processed for Southern Blot as previously described (48). TRE probe and SV40 probe were both excised from pTetO-β2VL vector and labeled with [α-^{32}P]dCTP (Amersham Biosciences, Piscataway, NJ, USA) by random priming (Rediprime II, Amersham Biosciences, Piscataway, NJ, USA); filters were then exposed to KODAK autoradiograph film (Amersham Biosciences, Piscataway, NJ, USA) at −70°C with intensifying screen for 4–96 h and in the end films were developed.

For the quantification of transgene copy number insertion, gDNA was digested with *Dpn*II restriction enzyme generating fragments of different length for the endogenous *Chrnb2* gene and *Chrnb2*^{V287L} transgene (1747 and 1143 bp, respectively). Increasing amounts of digested DNA (2, 4 and 8 μg) were loaded on a 0.8% agarose gel in TAE buffer to directly compare endogenous gene versus transgene band intensity. Endogenous gene and transgene were detected using a probe on exon 5, excised from pTetO-β2VL vector with *Nde*I–*Sph*I enzymes. Blot, hybridization and detection were performed as described earlier.

To determine transgene site of insertion, gDNA from tails of Tg(TRE-*Chrnb2*^{V287L}) lines was digested overnight with 50 U of *Mse*I restriction enzyme cutting in the SV40 polyA sequence and ligated with T4 DNA ligase after purification. The self-ligated circular DNA was linearized with *Hin*fI enzyme, then amplified by inverse PCR with outwardly facing primers within the transgene sequence (forward primer: CAGGTCA ACAGGCGGTAAC; reverse primer: GCACAGATAGCGTG GTCCG) at 94°C for 1 min and 30 s, 34 cycles at 94°C for 25 s, 53°C for 20 s, 65°C for 50s and 65°C for 10 min. One microliter of inverse PCR product was then amplified with nested primers (forward: CCTGGCGGACGGGAAGTA; reverse: CAGGACGACGAGGCTTGC) at 94°C for 1 min and 30 s, 36 cycles at 94°C for 25 s, 55°C for 20 s, 65°C for 45s and 65°C for 10 min.

Nested PCR products were separated on 1.5% agarose gel and the specific transgene bands purified and sequenced (MegaBACE 1000 analyzer). Site of insertion of the transgene in each transgenic line was unambiguously identified by alignment (BLAST).

Analysis of transgene expression

Total RNA was extracted from tissues of 2-month-old mice and from brains of P1–2 mice by Trizol method and subsequently treated with DNase I (Invitrogen, Carlsbad, CA, USA) for 15 min at room temperature to eliminate gDNA. RNA was reverse transcribed using random hexamers SuperScript® First-Strand Synthesis System (Invitrogen, Carlsbad, CA, USA) according to the manufacturer's instructions. RT-minus control was included in each reaction to control the absence of gDNA contamination in RNA preparations. Endogenous and transgenic *Chrnb2* cDNA was amplified using forward primer on exon 5 (TGGACATCACCTACGA CTTC) and reverse primer on exon 6 (CGTATTTCCAATC CTCCCTC) at 94°C for 1 min and 30 s, 36 cycles at 94°C for 25 s, 55°C for 20 s, 65°C for 45s and 65°C for 10 min. The PCR product of 700 bp was subsequently digested with transgene-specific restriction enzyme *Hin*fI and then run on a 1.5% agarose gel in TAE buffer; intensity of bands corresponding to the endogenous gene (uncut product: 700 bp band) and to the transgene (cut products: 500+200 bp bands) was quantified by fluorescence detection (Typhoon

Downloaded from hmg.oxfordjournals.org at (D) Fukuoka U Med on October 4, 2010

Scanner, Amersham Biosciences, Piscataway, NJ, USA) and scanned image analysis (ImageQuant, Amersham Biosciences, Piscataway, NJ, USA).

For the analysis of brain regional expression, total RNA was extracted from cortex, thalamus, caudate-putamen, hippocampus, hypothalamus, brain stem and cerebellum of Tg(tTA:*Chrnb2*^{V287L}). Mice were sacrificed by cervical dislocation after anesthesia and the whole brain removed. Brain was processed with a tissue chopper (McIlwain Tissue Chopper, Vibratom) and areas dissected under a stereomicroscope. Total RNA was reverse transcribed as described and *Chrnb2* cDNA amplified by PCR. Because of the small amount of RNA extracted from brain areas, the PCR strategy described earlier was preceded by a first amplification with external primers (forward CTGGACCTACGACCGCACT GAGA and reverse (GATCCAGAGGAACAGGCGGTCGA, at 94°C for 1 min and 30 s, 42 cycles at 94°C for 25 s, 62°C for 20 s, 65°C for 1 min and 65°C for 10 min). Detection and comparison of endogenous gene versus transgene expression were performed as described earlier.

Binding assay, immunoblotting and immunoprecipitation

Cortex, hippocampus, caudate-putamen and thalamus of wild-type, Tg(PrnP-tTA) and Tg(tTA:*Chrnb2*^{V287L}) mice were dissected, immediately frozen in liquid nitrogen and stored at −80°C for later use. In each experiment, tissues were homogenized in an excess of 50 mM Na phosphate pH 7.4, 1 M NaCl, 2 mM EDTA, 2 mM EGTA and 2 mM phenylmethylsulfonylfluoride and the protein content of the membranes measured using the BCA protein assay (Pierce, Rockford, IL, USA) with bovine serum albumin as standard.

Binding experiments were carried out by incubating aliquots of membrane homogenates with (+/−)^{3}H-epibatine (^{3}H-epi; specific activity of 70.6 Ci/mmol, purchased from NEN, Boston, USA) 2 nM at 4°C overnight in the presence of 2 μM αBungarotoxin (Sigma-Aldrich, Milan, Italy), to prevent ^{3}H-epi binding to the subtypes containing the α7 subunit. Non-specific binding (averaging 5–10% of total binding) was determined in parallel by means of incubation in the presence of 100 nM unlabeled epibatidine (RBI, Natick, MA). After incubation, the samples were filtered on a GFC filter soaked in 0.5% polyethylenimine, washed with 15 ml of 10 mM Na phosphate pH 7.4, plus 50 mM NaCl and counted in a β counter.

^{125}I-αBungarotoxin binding experiments were performed by incubating membranes overnight with saturating concentration of ^{125}I-αBungarotoxin (^{125}I-αBgtx; specific activity of 220 Ci/mmol, purchased from Amersham Biosciences, Piscataway, NJ, USA) at 20°C (5–8 nM). 2 mg/ml bovine serum albumin was added to the suspension buffer. Specific radioligand binding was defined as total binding minus non-specific binding determined in the presence of 1 μM cold αBungarotoxin.

Comparison of specific binding (mean ± s.e.m. of four experiments performed on the different areas) between genotypes was analyzed by one-way ANOVA followed by Tukey's multiple comparison *post hoc* test.

Wild-type or V287L mutant receptor constructs were transfected in HeLa cells for saturation binding and inhibition experiments. Membrane preparation from transfected cells were incubated with ^{3}H-epi (NEN, Boston, MA) at concentration ranging from 0.005–5 nM for saturation binding. For inhibition experiments, membranes were incubated 30 min with increasing concentrations (1 pM to 10 μM) of unlabeled nicotine before adding ^{3}H-epi at the K_D concentration. Incubation was prolonged for 3 h at RT. Non-specific binding was measured in the presence of 200 nM unlabeled epi. The experimental data obtained from the saturation binding experiments were analyzed by non-linear least square procedure using the LIGAND program as described in (52). The calculated binding parameters were obtained on two independent experiments.

The K_i values of nicotine were determined by means of the LIGAND program using the data obtained from two independent competition experiments and compared by means of the *F*-test.

In western blot analysis, 5–10 μg of protein obtained from membranes of each area were dissolved 1:1 (vol/vol) with Laemmli buffer and then underwent SDS–PAGE using 9% acrylamide. The proteins were electrophoretically transferred to nitrocellulose membranes (Schleicher and Schuell, Dassel, Germany) with 0.45 mm pores. The blots were blocked overnight with 5% non-fat milk in Tris buffered saline (TBS), washed in a buffer containing 5% non-fat-milk and 0.3% Tween 20 in TBS, incubated for 2 h with 5 μg/ml of subunit-specific polyclonal antibodies, then incubated with the appropriate peroxidase conjugated secondary antibodies. After another series of washes, peroxidase was detected using a chemiluminescent substrate (Pierce, Rockford, IL, USA).

The intensity of the western blot bands was acquired using an Epson 4500 scanner and optical density analyzed using NIH Image J software (National Technical Information Service, Springfields, VA, USA). Values are expressed as fold variations versus wt.

For immunoprecipitation experiments 2% Triton X-100 extracts were prepared from membranes as described previously (53). Extracts were labeled with 2 nM ^{3}H-epi and then incubated with a saturating concentration of anti-subunit affinity purified IgG (anti-α2, -α3, -α4, -α5, -α6, -β2, -β3, -β4 subunits). Each immunoprecipitate was recovered by incubating the samples with beads containing bound anti-rabbit goat IgG (Technogenetics, Milan, Italy) and analyzed by one-way ANOVA followed by Tukey's multiple comparison *post hoc* test.

Behavioral analysis

Sensory-motor function of mutant mice compared with controls was assessed by SHIRPA protocol primary screening (54). Briefly, undisturbed behavior of each animal was first observed in its own home cage: body position, spontaneous activity and respiration rate were recorded, assigning a score to each behavior. In addition, manifestations of tremors, bizarre behaviors, stereotypes or convulsions were checked at this stage of the protocol. Thereafter mice were transferred individually to a new arena and were tested for transfer arousal, palpebral closing, piloerection, gait, pelvic and tail elevation, touch escape and positional passivity. There followed a sequence of manipulations using tail suspension and

Downloaded from hmg.oxfordjournals.org at (D) Fukuoka U Med on October 4, 2010

a grid across the width of the arena: animals were scored for trunk curl, limb grasping and grip strength. To complete the assessment, the animals were restrained in a supine position to record autonomic behaviors (heart rate, skin color, limb and abdominal tone, lacrimation, salivation) prior to measurement of the righting reflex after flip of the animal. Vocalizations and irritability (during supine restrain) were also recorded. Fear was assessed based on reaction to transfer to a new environment.

EEG analysis

Mice were anesthetized with intraperitoneal (i.p.) injection of 5% chloral hydrate dissolved in saline and given in a volume of 10 ml/kg body mass. Four screw electrodes (Bilaney Consultants GMBH, Dusseldorf, Germany) were inserted bilaterally through the skull over cortex (anteroposterior, +2.0–3.0 mm; left–right 2.0 mm from bregma) according to brain atlas coordinates (55); a further electrode was placed into the nasal bone as ground. The five electrodes were connected to a pedestal (Bilaney, Dusseldorf, Germany) and fixed with acrylic cement (Palavit, New Galetti and Rossi, Milan, Italy). The animals were allowed a week of recovery from surgery before starting the experiment and acclimatized to a sound-attenuated Faraday chamber for a period of 3 days. For the assessment of basal cerebral activity, freely moving mice were recorded continuously for 24 h using PowerLab System (ADInstruments, Castle Hill, Australia). EEG traces were sampled at 100 Hz.

EEG recordings of doxycycline-treated animals were performed as described earlier, after 1–3 weeks of doxycycline treatment (1 mg/ml in drinking water with 5% sucrose to mask the bitter taste) changed every 2 days. After EEG recordings mice were sacrificed and transgene silencing was verified by RT–PCR.

In experiments involving mice treated with doxycycline since embryonic stage, doxycycline (1 mg/ml) was administrated from E1 to P15 in mothers' drinking water. Tg(tTA:*Chrnb2*^{V287L}) mice were then recorded by 24 h EEG, as previously described, at 4 months of age. After recordings mice were sacrificed and brain processed for RT–PCR as described earlier to verify transgene switch on.

For EEG analysis after antiepileptic treatment carbamazepine was suspended in 1% Tween80 and administered daily for 1 week via i.p. at the dose of 30 mg/kg in a volume of 10 ml/kg body mass. Twenty-four hour EEG recording was performed both after the first acute treatment and after chronic treatment on the seventh day.

For each 24-h EEG recording, the histogram of the maximum positive increments over overlapping 20 ms windows was derived. The expected distribution tail for normal EEG activity decreases exponentially (56), thus forbidding large increments. In the presence of abnormal events, as spikes, because of the large fast EEG increments, histogram decays slower and shows a 'heavy-tailed' behavior; in a log-linear plot it deviates from the exponential distribution represented as a straight line.

By prolonging the linear segment of the distribution tail, it was possible to determine a cut-off value for each 24-h recording. Above this threshold, the potential increments within 20 ms were considered as spikes and an estimation of the number of their occurrences could be obtained. The linear fitting was accomplished by least squares method on a window of 40 ms centered on the vanishing value of the second derivative of the histogram (about 50 ms).

Seizures were identified automatically as rapid sequence of spikes (at least nine events over-threshold at a distance less than 1 s) and local increase of signal power, and then verified visually.

Spectral profiles for delta (0.5–4 Hz) and theta (4–8 Hz) frequency bands were obtained along the 24 h monitoring. For each 60 s epoch, the spectrum was estimated according to the Welch method (with a Hamming window of 10 s) and the content of both delta and theta frequencies was expressed as a percentage of the total EEG power (computed in the 0–30 Hz range).

EEG power density values were analyzed in each frequency bin (0.1 Hz resolution) by one-way ANOVA and *post hoc* tests (with 'Tukey-Kramer' correction for multiple comparisons) to evaluate the significance level of differences between genotypes.

For the analysis of epileptic events occurrence during delta epochs, the *P*-value was determined by applying the hypergeometric distribution as the probability to randomly select a number of 4 s epochs containing spikes in the total number of epochs of the entire recording and get the found proportion of epochs where delta /theta ratio was at least 2. Analyses were made in the Matlab programming environment (The Mathworks, Natick, MA).

SUPPLEMENTARY MATERIAL

Supplementary Material is available at *HMG* online.

ACKNOWLEDGEMENTS

We want to thank M. Zucconi and M. Manconi for critical discussion, E. Montini for i-PCR support and Michele Zoli for receptor radioligand binding support. We greatly acknowledge S.B. Prusiner and A. Servadio for kindly providing the PrnP-tTA/F959 responsive line.

Conflict of Interest statement. None declared.

FUNDING

We thank the Fondazione Mariani and the Italian Minister of Health for supporting this work. C.G. was supported by EU-Neurocypres, Fondazione Cariplo (2006/0779/109251) and Compagnia San Paolo (2005-1964 to C.G.) grants.

REFERENCES

1. Hirtz, D., Thurman, D.J., Gwinn-Hardy, K., Mohamed, M., Chaudhuri, A.R. and Zalutsky, R. (2007) How common are the 'common' neurologic disorders? *Neurology*, **68**, 326–337.
2. Heron, S.E., Scheffer, I.E., Berkovic, S.F., Dibbens, L.M. and Mulley, J.C. (2007) Channelopathies in idiopathic epilepsy. *Neurotherapeutics*, 4, 295–304.
3. Scheffer, I.E., Bhatia, K.P., Lopes-Cendes, I., Fish, D.R., Marsden, C.D., Andermann, E., Andermann, F., Desbiens, R., Keene, D., Cendes, F. *et al.* (1995) Autosomal dominant nocturnal frontal lobe epilepsy. A distinctive clinical disorder. *Brain*, **118**, 61–73.

Downloaded from hmg.oxfordjournals.org at (D) Fukuoka U Med on October 4, 2010

4. Hayman, M., Scheffer, I.E., Chinvarun, Y., Berlangieri, S.U. and Berkovic, S.F. (1997) Autosomal dominant nocturnal frontal lobe epilepsy: demonstration of focal frontal onset and intrafamilial variation. *Neurology*, **49**, 969–975.
5. Steinlein, O.K., Mulley, J.C., Propping, P., Wallace, R.H., Phillips, H.A., Sutherland, G.R., Scheffer, I.E. and Berkovic, S.F. (1995) A missense mutation in the neuronal nicotinic acetylcholine receptor alpha 4 subunit is associated with autosomal dominant nocturnal frontal lobe epilepsy. *Nat. Genet.*, **11**, 201–203.
6. Steinlein, O.K., Magnusson, A., Stoodt, J., Bertrand, S., Weiland, S., Berkovic, S.F., Nakken, K.O., Propping, P. and Bertrand, D. (1997) An insertion mutation of the CHRNA4 gene in a family with autosomal dominant nocturnal frontal lobe epilepsy. *Hum. Mol. Genet.*, **6**, 943–947.
7. Hirose, S., Iwata, H., Akiyoshi, H., Kobayashi, K., Ito, M., Wada, K., Kaneko, S. and Mitsudome, A. (1999) A novel mutation of CHRNA4 responsible for autosomal dominant nocturnal frontal lobe epilepsy. *Neurology*, **53**, 1749–1753.
8. Aridon, P., Marini, C., Di Resta, C., Brilli, E., De Fusco, M., Politi, F., Parrini, E., Manfredi, I., Pisano, T., Pruna, D. *et al.* (2006) Increased sensitivity of the neuronal nicotinic receptor alpha 2 subunit causes familial epilepsy with nocturnal wandering and ictal fear. *Am. J. Hum. Genet.*, **79**, 342–350.
9. De Fusco, M., Becchetti, A., Patrignani, A., Annesi, G., Gambardella, A., Quattrone, A., Ballabio, A., Wanke, E. and Casari, G. (2000) The nicotinic receptor beta 2 subunit is mutant in nocturnal frontal lobe epilepsy. *Nat. Genet.*, **26**, 275–276.
10. Phillips, H.A., Favre, I., Kirkpatrick, M., Zuberi, S.M., Goudie, D., Heron, S.E., Scheffer, I.E., Sutherland, G.R., Berkovic, S.F., Bertrand, D. *et al.* (2001) CHRNB2 is the second acetylcholine receptor subunit associated with autosomal dominant nocturnal frontal lobe epilepsy. *Am. J. Hum. Genet.*, **68**, 225–231.
11. Bertrand, D., Elmslie, F., Hughes, E., Trounce, J., Sander, T., Bertrand, S. and Steinlein, O.K. (2005) The CHRNB2 mutation I312M is associated with epilepsy and distinct memory deficits. *Neurobiol. Dis.*, **20**, 799–804.
12. Wonnacott, S., Irons, J., Rapier, C., Thorne, B. and Lunt, G.G. (1989) Presynaptic modulation of transmitter release by nicotinic receptors. *Prog. Brain Res.*, **79**, 157–163.
13. Bertrand, D., Picard, F., Le Hellard, S., Weiland, S., Favre, I., Phillips, H., Bertrand, S., Berkovic, S.F., Malafosse, A. and Mulley, J. (2002) How mutations in the nAChRs can cause ADNFLE epilepsy. *Epilepsia*, **43** (Suppl. 5), 112–122.
14. Rodrigues-Pinguet, N., Jia, L., Li, M., Figl, A., Klaassen, A., Truong, A., Lester, H.A. and Cohen, B.N. (2003) Five ADNFLE mutations reduce the Ca2+ dependence of the mammalian alpha4beta2 acetylcholine response. *J. Physiol.*, **550**, 11–26.
15. Weiland, S., Witzemann, V., Villarroel, A., Propping, P. and Steinlein, O. (1996) An amino acid exchange in the second transmembrane segment of a neuronal nicotinic receptor causes partial epilepsy by altering its desensitization kinetics. *FEBS Lett.*, **398**, 91–96.
16. Klaassen, A., Glykys, J., Maguire, J., Labarca, C., Mody, I. and Boulter, J. (2006) Seizures and enhanced cortical GABAergic inhibition in two mouse models of human autosomal dominant nocturnal frontal lobe epilepsy. *Proc. Natl Acad. Sci. USA*, **103**, 19152–19157.
17. Teper, Y., Whyte, D., Cahir, E., Lester, H.A., Grady, S.R., Marks, M.J., Cohen, B.N., Fonck, C., McClure-Begley, T., McIntosh, J.M. *et al.* (2007) Nicotine-induced dystonic arousal complex in a mouse line harboring a human autosomal-dominant nocturnal frontal lobe epilepsy mutation. *J. Neurosci.*, **27**, 10128–10142.
18. Gossen, M. and Bujard, H. (1992) Tight control of gene expression in mammalian cells by tetracycline-responsive promoters. *Proc. Natl Acad. Sci. USA*, **89**, 5547–5551.
19. Tremblay, P., Meiner, Z., Galou, M., Heinrich, C., Petromilli, C., Lisse, T., Cayetano, J., Torchia, M., Mobley, W., Bujard, H. *et al.* (1998) Doxycycline control of prion protein transgene expression modulates prion disease in mice. *Proc. Natl Acad. Sci. USA*, **95**, 12580–12585.
20. Tremblay, P., Bouzamondo-Bernstein, E., Heinrich, C., Prusiner, S.B. and DeArmond, S.J. (2007) Developmental expression of PrP in the post-implantation embryo. *Brain Res.*, **1139**, 60–67.
21. Dobie, K., Mehtali, M., McClenaghan, M. and Lathe, R. (1997) Variegated gene expression in mice. *Trends Genet.*, **13**, 127–130.
22. Frey, H.H. and Yanz, D. (1985) *Handbook of Experimental Pharmacology*. Springer, Berlin.
23. Perea, J., Robertson, A., Tolmachova, T., Muddle, J., King, R.H., Ponsford, S., Thomas, P.K. and Huxley, C. (2001) Induced myelination and demyelination in a conditional mouse model of Charcot-Marie-Tooth disease type 1A. *Hum. Mol. Genet.*, **10**, 1007–1018.
24. Gotti, C. and Clementi, F. (2004) Neuronal nicotinic receptors: from structure to pathology. *Prog. Neurobiol.*, **74**, 363–396.
25. Wonnacott, S. (1997) Presynaptic nicotinic ACh receptors. *Trends Neurosci.*, **20**, 92–98.
26. Alkondon, M., Pereira, E.F. and Albuquerque, E.X. (1998) alpha-bungarotoxin- and methyllycaconitine-sensitive nicotinic receptors mediate fast synaptic transmission in interneurons of rat hippocampal slices. *Brain Res.*, **810**, 257–263.
27. Marini, C. and Guerrini, R. (2007) The role of the nicotinic acetylcholine receptors in sleep-related epilepsy. *Biochem. Pharmacol.*, **74**, 1308–1314.
28. Gotti, C., Moretti, M., Meinerz, N., Clementi, F., Gaimarri, A., Collins, A.C. and Marks, M.J. (2008) Partial deletion of the nicotinic cholinergic receptor {alpha}4 and {beta}2 subunit genes changes the acetylcholine sensitivity of receptor mediated 86Rb+ efflux in cortex and thalamus and alters relative expression of {alpha}4 and {beta}2 subunits. *Mol. Pharmacol.*
29. Kuryatov, A., Onksen, J. and Lindstrom, J. (2008) Roles of accessory subunits in alpha4beta2(*) nicotinic receptors. *Mol. Pharmacol.*, **74**, 132–143.
30. Steriade, M., McCormick, D.A. and Sejnowski, T.J. (1993) Thalamocortical oscillations in the sleeping and aroused brain. *Science*, **262**, 679–685.
31. Steriade, M., Dossi, R.C. and Nunez, A. (1991) Network modulation of a slow intrinsic oscillation of cat thalamocortical neurons implicated in sleep delta waves: cortically induced synchronization and brainstem cholinergic suppression. *J. Neurosci.*, **11**, 3200–3217.
32. Ferrillo, F., Beelke, M. and Nobili, L. (2000) Sleep EEG synchronization mechanisms and activation of interictal epileptic spikes. *Clin. Neurophysiol.*, **111** (Suppl. 2), S65–S73.
33. Steriade, M. and Contreras, D. (1995) Relations between cortical and thalamic cellular events during transition from sleep patterns to paroxysmal activity. *J. Neurosci.*, **15**, 623–642.
34. Molow, B.A., Lin, X., Kushwaha, R. and Aldrich, M.S. (1998) Interictal spiking increases with sleep depth in temporal lobe epilepsy. *Epilepsia*, **39**, 1309–1316.
35. Oldani, A., Zucconi, M., Asselta, R., Modugno, M., Bonati, M.T., Dalpra, L., Malcovati, M., Tenchini, M.L., Smirne, S. and Ferini-Strambi, L. (1998) Autosomal dominant nocturnal frontal lobe epilepsy. A video-polysomnographic and genetic appraisal of 40 patients and delineation of the epileptic syndrome. *Brain*, **121**, 205–223.
36. Provini, F., Plazzi, G., Tinuper, P., Vandi, S., Lugaresi, E. and Montagna, P. (1999) Nocturnal frontal lobe epilepsy. A clinical and polygraphic overview of 100 consecutive cases. *Brain*, **122**, 1017–1031.
37. Chevassus-au-Louis, N., Baraban, S.C., Gaiarsa, J.L. and Ben-Ari, Y. (1999) Cortical malformations and epilepsy: new insights from animal models. *Epilepsia*, **40**, 811–821.
38. Guerrini, R., Dobyns, W.B. and Barkovich, A.J. (2008) Abnormal development of the human cerebral cortex: genetics, functional consequences and treatment options. *Trends Neurosci.*, **31**, 154–162.
39. Role, L.W. and Berg, D.K. (1996) Nicotinic receptors in the development and modulation of CNS synapses. *Neuron*, **16**, 1077–1085.
40. Zoli, M., Le Novere, N., Hill, J.A. Jr and Changeux, J.P. (1995) Developmental regulation of nicotinic ACh receptor subunit mRNAs in the rat central and peripheral nervous systems. *J. Neurosci.*, **15**, 1912–1939.
41. Tribollet, E., Bertrand, D., Marguerat, A. and Raggenbass, M. (2004) Comparative distribution of nicotinic receptor subtypes during development, adulthood and aging: an autoradiographic study in the rat brain. *Neuroscience*, **124**, 405–420.
42. Greenberg, M.E., Ziff, E.B. and Greene, L.A. (1986) Stimulation of neuronal acetylcholine receptors induces rapid gene transcription. *Science*, **234**, 80–83.
43. Zheng, J.Q., Felder, M., Connor, J.A. and Poo, M.M. (1994) Turning of nerve growth cones induced by neurotransmitters. *Nature*, **368**, 140–144.
44. Rossi, F.M., Pizzorusso, T., Porciatti, V., Marubio, L.M., Maffei, L. and Changeux, J.P. (2001) Requirement of the nicotinic acetylcholine receptor beta 2 subunit for the anatomical and functional development of the visual system. *Proc. Natl Acad. Sci. USA*, **98**, 6453–6458.

Downloaded from hmg.oxfordjournals.org at (D) Fukuoka U Med on October 4, 2010

45. King, S.L., Marks, M.J., Grady, S.R., Caldarone, B.J., Koren, A.O., Mukhin, A.G., Collins, A.C. and Picciotto, M.R. (2003) Conditional expression in corticothalamic efferents reveals a developmental role for nicotinic acetylcholine receptors in modulation of passive avoidance behavior. *J. Neurosci.*, **23**, 3837–3843.
46. Le Magueresse, C., Safiulina, V., Changeux, J.P. and Cherubini, E. (2006) Nicotinic modulation of network and synaptic transmission in the immature hippocampus investigated with genetically modified mice. *J. Physiol.*, **576**, 533–546.
47. Liu, Z., Neff, R.A. and Berg, D.K. (2006) Sequential interplay of nicotinic and GABAergic signaling guides neuronal development. *Science*, **314**, 1610–1613.
48. Walker, M.C., White, H.S. and Sander, J.W. (2002) Disease modification in partial epilepsy. *Brain*, **125**, 1937–1950.
49. Sutor, B. and Zolles, G. (2001) Neuronal nicotinic acetylcholine receptors and autosomal dominant nocturnal frontal lobe epilepsy: a critical review. *Pflugers Arch.*, **442**, 642–651.
50. Combi, R., Dalpra, L., Tenchini, M.L. and Ferini-Strambi, L. (2004) Autosomal dominant nocturnal frontal lobe epilepsy–a critical overview. *J. Neurol.*, **251**, 923–934.
51. Zoli, M., Moretti, M., Zanardi, A., McIntosh, J.M., Clementi, F. and Gotti, C. (2002) Identification of the nicotinic receptor subtypes expressed on dopaminergic terminals in the rat striatum. *J. Neurosci.*, **22**, 8785–8789.
52. Munson, P.J. and Rodbard, D. (1980) Ligand: a versatile computerized approach for characterization of ligand-binding systems. *Anal. Biochem.*, **107**, 220–239.
53. Gotti, C., Moretti, M., Zanardi, A., Gaimarri, A., Champtiaux, N., Changeux, J.P., Whiteaker, P., Marks, M.J., Clementi, F. and Zoli, M. (2005) Heterogeneity and selective targeting of neuronal nicotinic acetylcholine receptor (nAChR) subtypes expressed on retinal afferents of the superior colliculus and lateral geniculate nucleus: identification of a new native nAChR subtype alpha3beta2(alpha5 or beta3) enriched in retinocollicular afferents. *Mol. Pharmacol.*, **68**, 1162–1171.
54. Rogers, D.C., Fisher, E.M., Brown, S.D., Peters, J., Hunter, A.J. and Martin, J.E. (1997) Behavioral and functional analysis of mouse phenotype: SHIRPA, a proposed protocol for comprehensive phenotype assessment. *Mamm. Genome*, **8**, 711–713.
55. Paxinos, G. and Franklin, K.B.J. (2004) *The Mouse Brain in Stereotaxic Coordinates*, San Diego.
56. White, A.M., Williams, P.A., Ferraro, D.J., Clark, S., Kadam, S.D., Dudek, F.E. and Staley, K.J. (2006) Efficient unsupervised algorithms for the detection of seizures in continuous EEG recordings from rats after brain injury. *J. Neurosci. Methods*, **152**, 255–266.

Downloaded from hmg.oxfordjournals.org at (D) Fukuoka U Med on October 4, 2010